



HAL
open science

On the time sequence of the transient flow boiling crisis at high subcooling

Raksmey Nop, Marie-Christine Duluc, Nicolas Dorville, Artyom Kossolapov,
Florian Chavagnat, Matteo Bucci

► **To cite this version:**

Raksmey Nop, Marie-Christine Duluc, Nicolas Dorville, Artyom Kossolapov, Florian Chavagnat, et al.. On the time sequence of the transient flow boiling crisis at high subcooling. 15th International Conference on Heat Transfer, Fluid Mechanics and Thermodynamics, Jul 2021, (Online), France. pp.1736. cea-04440565

HAL Id: cea-04440565

<https://cea.hal.science/cea-04440565>

Submitted on 6 Feb 2024

HAL is a multi-disciplinary open access archive for the deposit and dissemination of scientific research documents, whether they are published or not. The documents may come from teaching and research institutions in France or abroad, or from public or private research centers.

L'archive ouverte pluridisciplinaire **HAL**, est destinée au dépôt et à la diffusion de documents scientifiques de niveau recherche, publiés ou non, émanant des établissements d'enseignement et de recherche français ou étrangers, des laboratoires publics ou privés.

ON THE TIME SEQUENCE OF THE TRANSIENT FLOW BOILING CRISIS AT HIGH SUBCOOLING

R. Nop^{123*}, M.-C. Duluc²⁴, N. Dorville¹, A. Kossolapov³, F. Chavagnat³ and M. Bucci³

¹Université Paris-Saclay, CEA, Service de thermo-hydraulique et de mécanique des fluides, 91191, Gif-sur-Yvette, France.

* raksmy.nop@cea.fr

²Université Paris-Saclay, CNRS, Laboratoire interdisciplinaire des sciences du numérique, 91405, Orsay, France..

³Department of Nuclear Science and Engineering, Massachusetts Institute of Technology, Cambridge MA 02139, USA.

⁴Conservatoire National des Arts et Métiers, 75003, Paris, France

NOMENCLATURE

a	[$m^2.s^{-1}$]	Thermal diffusivity
b	[$J.m^{-2}.K^{-1}.s^{-1/2}$]	Thermal effusivity
q''_w	[$W.m^{-2}$]	Heat flux transferred to water
q^*	[-]	Normalized heat flux
t	[s]	Time
t^*	[-]	Normalized Time
T_w	[K]	Wall temperature

Greek letter		
ΔT_{sub}	[K]	Subcooling temperature
Δt^*	[-]	Normalized duration of the two-phase regime
τ	[s]	exponential period
Θ	[-]	Normalized temperature

Subscripts	
CHF	Critical Heat Flux
ONB	Onset on Nucleate Boiling
ref	Normalization quantity
s	Sapphire
l	Liquid

ABSTRACT

Transient flow boiling crisis at atmospheric pressure in highly-subcooled water (50, 75 K) is investigated with Reynolds numbers up to 35000. An exponential heat input is delivered with an escalation period τ covering the range 5 – 500 ms. We present the results using normalized values for time, wall temperature and the heat flux transferred to the water. The period τ and the subcooling are shown to have a major impact on transient boiling crisis while the Reynolds number has a minor effect. The time required for boiling crisis to happen is mainly spent in the single-phase heat transfer regime due to the high degree of subcooling. The time duration of the two-phase flow regime represents only a small part of the total duration and tends to zero as the power escalation period is reduced.

INTRODUCTION

In case of a reactivity insertion accident in an experimental nuclear reactor, heat generation in the core can grow exponentially in time, with a power escalation period ranging from a few to a few hundreds milliseconds. Due to neutronic and thermo-hydraulic effects, boiling crisis may arise and possibly leads to an explosive reaction. Thus, a reliable prediction of the boiling crisis induced by fast transients is a key issue for nuclear safety.

Many works have been devoted to the subject since the pioneering studies such as the experimental reactors BORAX [1] or SPERT-IV [2]. In these experiments, only either integral quantities such as time-dependent core power, or local information such as temperature captured by thermocouples taped on the fuel plate were available. Boiling crisis is known to be triggered in a short time interval due to coalescence of neighboring bubbles which in turn generates a local dry spot. This process may occur almost anywhere on the heated wall and may therefore not be captured by small-size sensors. Consequently, it was easy to miss the real moment and location of the occurrence of the boiling crisis. The need to understand the mechanisms triggering to the boiling crisis led to the development of small-scale experiments. For instance, Kataoka et al. [3] investigated the transient boiling crisis using a heated vertical wire which enables the access of the time-dependent heat-flux and temperature. However, these information were space averaged on the wire. Recent studies, such as Kossolapov et al. [4], make use of high resolution measurement tools combined with high performance data analysis in order to understand the underlying physics. Therefore, detailed space and time information becomes available and finally enables to precisely determine how and when occurs the different events from the initiation of the transient to the boiling crisis.

Even though time is intrinsically present in all these studies, quantitative information is lacking about the time scales associated with the transient boiling crisis as well as its analysis. Yet, time information is a crucial element considering the need of an accurate prediction of the time delay before boiling crisis occurrence. Consequently, in the present communication, we present a time analysis of the transient flow boiling crisis at high subcooling, using the experimental data gathered in [4]. The objective is to identify the underlying physical mechanisms, the associated time scales and the governing parameters.

EXPERIMENTAL APPARATUS

Kossolapov et al. [4] realized a detailed experimental investigation of the subcooled flow boiling crisis. These experiments were conducted in a rectangular duct (1 x 3 cm²) using water with a subcooling up to 75 K and a Reynolds number up to 35,000. The heater is made of a 2 x 2 cm² square, 1mm-thick sapphire substrate coated by a film of ITO 0.7 μm thick (see Fig.1). The power input is generated by Joule effect in the ITO, electrically conductive, and the effective heating surface is a 1 x 1 cm² square. The exponential power escalation period τ of the heat input covers the range 5 – 500 ms.

The experiments were diagnosed by a high-speed IR camera (2,500 fps) located behind the heater. The latter is synchronized with a high-speed video camera (20,000 fps) placed front of the heater for visualization. The post-processing of the IR camera data, presented in [5], enables to measure the time-dependent distributions of the temperature at the wall and the heat flux transferred to the water. Their space averages $T_w(t)$ and $q''_w(t)$ are then also derived.

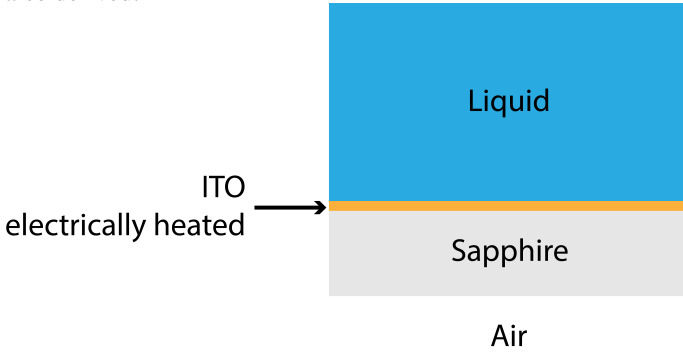


Figure 1: Sketch of the heater - not to scale

TIME DYNAMICS OF THE WALL TEMPERATURE AND THE HEAT FLUX

Normalized temperature and heat flux

The temperature of the liquid entering the test section is well below the saturation temperature, heat is transferred to the liquid by conduction and convection. When the heating process is fast -i.e. for small values of τ, heat transfer in the liquid is limited to a short distance from the wall. Heat diffusion is expected to be the dominating process. Disregarding end effects, the heat flux is transmitted in the single transverse direction. Accounting for both the liquid medium and the substrate, the heat diffusion problem may be solved analytically ([6], Eq.(12)). For an electrical heat flux input $q''_0 e^{t/\tau}$ released by the ITO and transferred to both the substrate and the water, we have:

$$\begin{aligned} T_w(t) - T_0 &= q''_0 e^{t/\tau} \left[\frac{b_s}{\sqrt{\tau}} \tanh \frac{L_s}{\sqrt{a_s \tau}} + \frac{b_l}{\sqrt{\tau}} \right]^{-1} \\ q''_w(t) &= q''_0 e^{t/\tau} b_l \left[b_s \tanh \frac{L_s}{\sqrt{a_s \tau}} + b_l \right]^{-1} \end{aligned} \quad (1)$$

This analysis suggests to plot the curves using non dimensional quantities defined as :

$$t^* = \frac{t}{\tau} \quad \Theta_w = \frac{T_w(t) - T_0}{\Delta T_{ref}} \quad q^* = \frac{q''_w(t)}{q''_{ref}} \quad (2)$$

with

$$\begin{aligned} \Delta T_{ref} &= \sqrt{\tau} \frac{q''_0}{\left[b_s \tanh \frac{L_s}{\sqrt{a_s \tau}} + b_l \right]} \\ q''_{ref} &= b_l \frac{q''_0}{\left[b_s \tanh \frac{L_s}{\sqrt{a_s \tau}} + b_l \right]} \end{aligned} \quad (3)$$

The reference quantities ΔT_{ref} and q''_{ref} depend on thermal properties of the substrate ($a_s = 6.8 \cdot 10^{-6} \text{ m}^2 \cdot \text{s}^{-1}$, $b_s = 9.6 \cdot 10^3 \text{ J} \cdot \text{m}^{-2} \cdot \text{K}^{-1} \cdot \text{s}^{-1/2}$) and of the liquid water ($b_l = 1.6 \cdot 10^3 \text{ J} \cdot \text{m}^{-2} \cdot \text{K}^{-1} \cdot \text{s}^{-1/2}$), the power escalation period (τ) and the initial value of the electrical power input (q''_0). They can therefore easily be transposed to other experiments. For this reason, we propose to represent the temperature and the heat flux transferred to the water using these specific reference quantities even though their relevance is *a priori* limited to the heat diffusion process.

Time evolution to transient boiling crisis

The normalized wall temperature and heat flux transferred to the water are presented in Fig.2 for three values of the escalation period τ = 5; 50; 500 ms and five sets of experimental conditions combining the subcooling $\Delta T_{sub} = 50; 75 \text{ K}$ and the Reynolds number $Re = 8,500; 25,000; 35,000$. These quantities are plotted from the beginning of the exponential excursion to CHF.

Each figure shows five curves which are in close coincidence. Time evolution of the heat flux shows two distinct processes. At early stages, heat transfer develops in the liquid phase. The heat flux increases slowly and regularly. Boiling inception occurs leading to a sharp increase of the heat flux until boiling crisis is triggered. The sudden change in the slope of the curve is due to the high efficiency of the boiling heat transfer. Indeed, the effusivity of water being significantly below the effusivity of sapphire, heat is preferentially transferred to the sapphire in single phase. This preference changes after ONB as boiling heat transfer is more efficient. Note that the change in the slope becomes smoother with the increase of τ, it is almost not visible for the cases at 500 ms. This behavior is due to two reasons. First, the term $\tanh(L_s/\sqrt{a_s \tau})$ decreases with τ, implying a better single-phase heat transfer to the water with the increase of the period. Secondly, the activation of the nucleation sites is significantly different between short and long periods: for long periods, the number of activated nucleation sites progressively increases and so the heat transfer whereas for short periods, nucleation sites are simultaneously activated on the heater

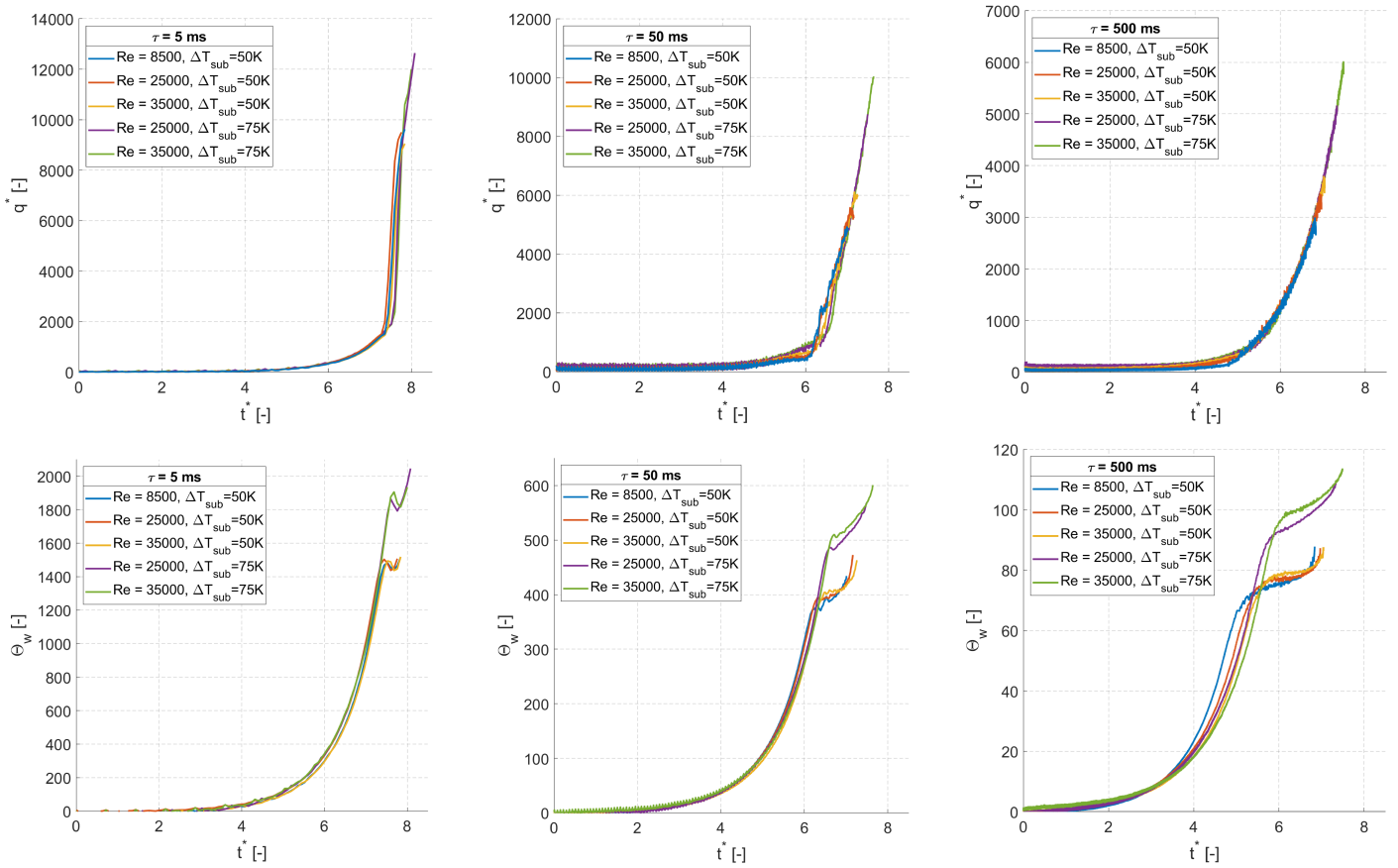


Figure 2: Normalized heat flux released to water q^* and normalized wall temperature Θ_w as a function of the normalized time t^* for $\tau = 5, 50, 500ms$ plotted from the beginning of the exponential power excursion to CHF.

increasing sharply the heat transfer at ONB. This is observed with both the high-speed visible and IR cameras.

One observes at a first glance that the normalized time required for boiling crisis to occur slightly depends on the time period τ , the subcooling or the Reynolds number. It ranges in the present case between 7 and 8. Naturally, this value is specific to the present experimental setup and in particular, strongly connected to the quantity q_0'' .

The parameter τ mainly impacts the relative duration of the single and two-phase regimes. Boiling onset occurs at a larger normalized time as the time period τ is reduced while the two-phase flow duration is shortened.

Now considering a fixed value of τ , the critical heat flux is seen to increase with the subcooling and with the Reynolds number. Fixing both the period and the subcooling, one observes the CHF to increase with the Reynolds number as the flow exerts a more efficient cooling in this case.

Remembering that the quantity q_{ref}'' does not depend on the subcooling neither on the Reynolds number (and slightly on the period), the vertical scale appears to be a relevant indicator to compare the CHF values.

Once the period τ fixed, the time evolution of the normalized wall temperature (lower row in Fig.2) also presents a close superimposition of the five curves. Similar trends are observed with the heat flux: the rise is steeper as the time period is reduced, the non-dimensional time duration associated to heat transfer in the single-phase regime increases while it is reduced for two-phase flow regime. The last period just before the occurrence of boiling crisis deserves a few comments. The curves measured for a subcooling of 75 K are correctly superimposed with those for 50 K in the single-phase regime then diverge after boiling incipience. This is not surprising remembering that the non dimensional temperature Θ_w was obtained starting from a heat diffusion model in the single liquid phase. A close superimposition between the curves is clearly perceptible for the escalation period $\tau = 5$ ms. For a large τ period associated with long time scales, convection effects are significant as revealed by the dispersed charts plotted in Fig.2- lower right.

Time evolution of the normalized wall temperature is changed after boiling inception. The slope drop is due to the high increase of the heat transfer coefficient. A large period τ leads to a smooth

increase : nucleate boiling develops progressively on the heated wall until dry spots occur leading to boiling crisis in a time delay of about two times the period τ . In contrast, a sharp temperature overshoot is observed at the boiling inception when the period is small (5 ms). Nucleation occurs homogeneously on the heater with a high density of activated nucleation sites. Boiling crisis is then triggered rapidly, in about half a period τ .

The time period $\tau = 50$ ms corresponds to an intermediate behavior as illustrated by Fig. 2 (middle column).

TIME SEQUENCE OF THE TRANSIENT CHF

Time evolution of the temperature and of the heat flux have been analyzed in regards of the different parameters. It is also interesting to quantitatively examine the duration of each regime during the transient. Indeed, from the beginning of the exponential power excursion to CHF, one could split the transient in two parts: single-phase and two-phase regimes. They are separated by ONB and the two-phase regime ends with CHF. One can plot the normalized time of each regime as a function of τ as presented in Fig.3.

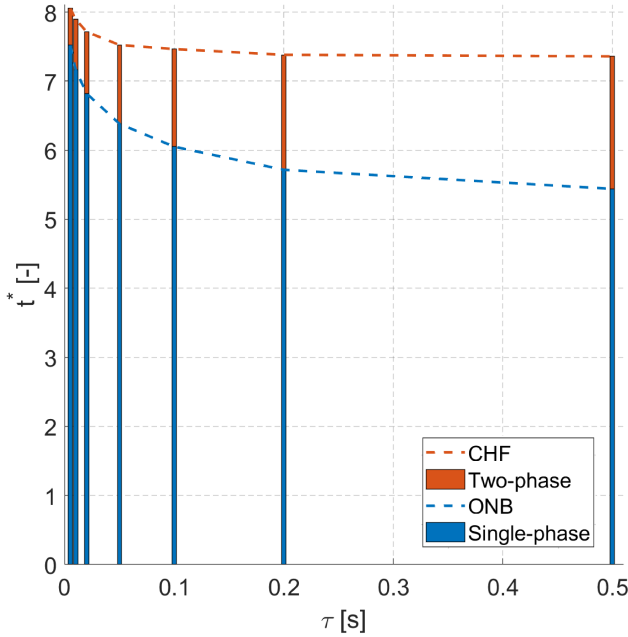


Figure 3: Overall time sequence of the exponential power excursion. The normalized time of the different occurrence and regime is presented as a function of the power escalation period τ . Example of the case $Re = 25000$ and $\Delta T_{sub} = 75$ K.

With this overview, it is interesting to note that at least three-fourth of the time is spent in single phase, *i.e.* 5 to 7 τ . This long time corresponds to the beginning of the exponential excursion where the temperature conditions are not reached for nucleation to start. Then, the time corresponding to two-phase flow reduces with the decrease of the power excursion period. For a small value of τ , time at boiling inception is large and

so the corresponding heat flux at the wall. Boiling occurs in the form of numerous tiny bubbles developing homogeneously along the heated wall in a very short time interval. In the following, a more quantitative insight on these different time characteristics is presented.

First of all, in Fig.4 the normalized time of ONB, t_{ONB}^* , is plotted as a function of τ for different conditions of subcooling and flow. The determination of the uncertainty is developed in appendix. For a given operating condition, t_{ONB}^* increases with the decrease τ . This reflects the fact that for a larger heat generation rate, the thermal boundary layer is thinner and delays the nucleation. Besides, Fig.4 shows that the impact of the subcooling prevails on the flow condition: the increase of ΔT_{sub} and Re delay nucleation, the latter having a smaller impact.

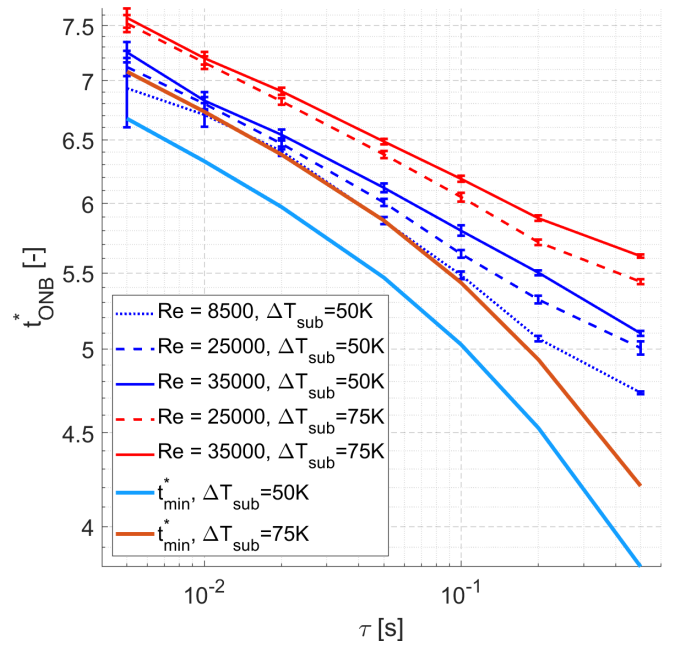


Figure 4: Dimensionless time of ONB and time t_{min}^* to reach the saturation temperature at the wall as function of the time period τ for the different operating conditions.

A quantitative minoration of t_{ONB}^* can be determined through a simple criterion. Indeed, since boiling can not be observed as long as the wall temperature is below saturation, a minimum time value can be computed considering the following criterion:

$$T_w(t_{min}) = T_{sat} \quad (4)$$

and the use of Eq. (1) gives the following analytic expression:

$$t_{min}^* = \frac{\Delta T_{sub}}{q_0''} \left[\frac{b_s}{\sqrt{\tau}} \tanh \frac{L_s}{\sqrt{a_s \tau}} + \frac{b_l}{\sqrt{\tau}} \right] \quad (5)$$

Plotted on Fig.4, this quantity cannot precisely catch t_{ONB}^* as a certain wall superheat is needed to trigger nucleation. The determination of this wall superheat needs the knowledge of the surface condition of the heating surface and also depends on the operating conditions and the escalation period [6]. However, it is interesting to note that this simple criterion catches parametric trends on the period τ and subcooling. We may observe a similar slope of t_{min}^* and t_{ONB}^* for small periods (*i.e.* less than 20 ms). An equal difference of 0.5 between the two subcooling is also observed showing that this time t_{min}^* yields a valuable quantitative information on the subcooling effect. This theoretical time also indicates that convection effects start to have a significant impact for τ longer than 20 ms where the discrepancy increases for higher period showing the increase of the flow condition influence. To summarize, time t_{min}^* , easily accessible from a theoretical point of view, overviews the impact of the operating parameters (τ , ΔT_{sub} , Re) and proposes a quantitative lower value of t_{ONB}^* .

Regarding CHF, the normalized time of CHF, t_{CHF}^* featured on Fig.5, follows a similar qualitative trend than the normalized time of ONB. For this set of experiments, it is interesting to notice that all CHF occur in an interval of time relatively restrained: between 7.7 and 8.2. However a more quantitative feature is not determined at this stage.

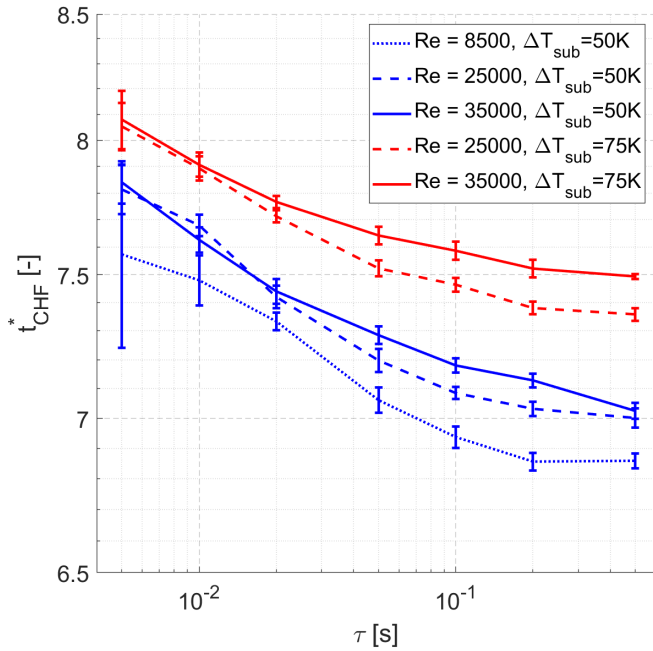


Figure 5: Dimensionless time of CHF as function of the time period τ

However, it is worth to examine the time spent in two-phase regime. Being the time between ONB and CHF, this quantity presented in Fig.6, is then defined as follow:

$$\Delta t^* = \frac{t_{CHF} - t_{ONB}}{\tau} \quad (6)$$

This normalized quantity is interesting as it allows to get rid of the initial conditions.

It reveals a better similarity between the different operating conditions, more than t_{CHF}^* . Indeed, for a given period τ , Δt^* are clustered in a small interval: as small as 0.2 for the short periods and 0.3 for the long ones. Besides, one can note that independently to the conditions, this quantity approximately follows a relatively simple trend as

$$\Delta t^* \propto \tau^{1/4} \quad (7)$$

Consequently, one expects this quantity to vanish when the power escalation period takes value smaller than 5 ms, and CHF would become concomitant with ONB. In other words, at significantly shorter escalation period, the large delay to nucleation, synonym of a large wall superheat, would generate such a explosive ONB that it would lead directly to boiling crisis.

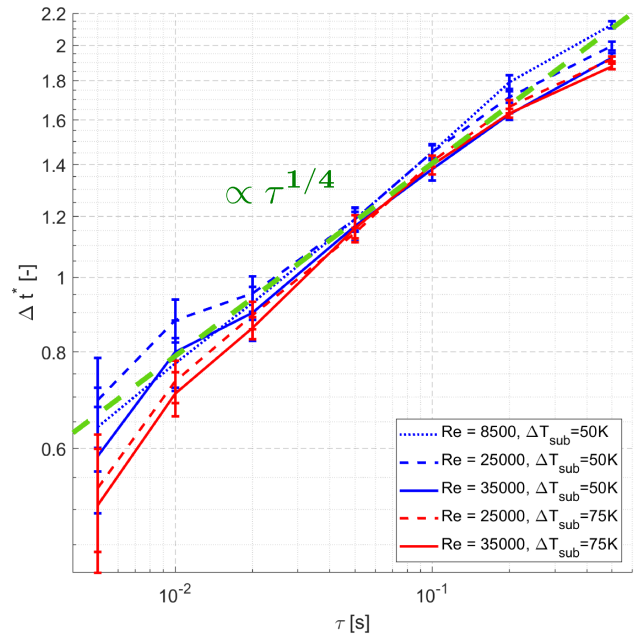


Figure 6: Dimensionless time spend in two-phase regime Δt^* as function of the time period τ for the different operating conditions.

CONCLUSION

The present communication investigates the time sequence of the transient flow boiling crisis at high subcooling using experimental data reported in Kossolapov et al. [4].

Time sequence of the transient CHF may be split in two stages: heat transfer is first realized in single-phase then in two-phase regime. At high subcooling, the whole duration of the process leading to boiling crisis, normalized with the escalation period τ , is almost insensible to the period. For a given experimental setup, it is mainly governed by the subcooling magnitude. It represents in the present case a duration of 7 to 8 τ . However, the corresponding physical times are very different and thus the energy released. One may infer from the present work that a small amount of energy remains near the wall at short periods whereas a large amount of energy is advected in the bulk at long periods. Future work should address the energy associated with the transient path leading to the CHF.

The whole duration of the time sequence is mostly consumed in the first stage as a large amount of heat is required to bring the highly subcooled liquid contacting the wall at the saturation temperature and as the exponential begins. For a subcooling equal to 75 K, this temporal contribution, which increases as the time period τ is reduced, consumes up to 90% of the total time. At short periods τ , heat diffusion in the liquid is the dominating process. A good estimate of the time needed for CHF to occur is achieved adding a couple of periods to a time quantity t_{min}^* . This particular time is determined theoretically from a heat diffusion model including thermal mass of the substrate.

Time duration for the two-phase flow regime is about 2 τ for the long periods but tends to zero as the time period τ is reduced, following a trend common to the different conditions. The progressive development of boiling crisis observed at large period turns gradually to a simultaneous triggering of ONB and CHF for the smallest periods due to the explosive nucleation. Lastly, a non-dimensional approach relying on a heat diffusion model including the solid contribution, appears to be a relevant tool for analyzing transient flow boiling crisis at high subcool-

ing. This is made possible because of the high subcoolings considered in the present work, most of the time-sequence is indeed consumed during the single-phase heat transfer.

REFERENCES

- [1] J. R. Dietrich, Experimental investigation of the self-limitation of power during reactivity transients in a subcooled, water-moderated reactor, *Argonne National Laboratory*, 1954.
- [2] J. G. Crocker, L. A. Stephan, Reactor Power Excursion Tests In The SPERT IV Facility, *Phillips Petroleum Company*, 1964.
- [3] I. Kataoka, A. Serizawa, A. Sakurai, Transient Boiling Heat Transfer under Forced Convection, *International Journal of Heat and Mass Transfer*, 1983.
- [4] A. Kossolapov, F. Chavagnat, R. Nop, N. Dorville, B. Phillips, J. Buongiorno, M. Bucci, The boiling crisis of water under exponentially escalating heat inputs in subcooled flow boiling at atmospheric pressure. *International Journal of Heat and Mass Transfer*, 2020.
- [5] M. Bucci, A. Richenderfer, G. Y. Su, T. McKrell, J. Buongiorno, A mechanistic IR calibration technique for boiling heat transfer investigations. *International Journal of Multiphase Flow*, 2016.
- [6] G. Y. Su, M. Bucci, T. McKrell, J. Buongiorno, Transient boiling of water under exponentially escalating heat inputs. Part I: Pool boiling. *International Journal of Heat and Mass Transfer*, 2016.

APPENDIX: UNCERTAINTY DETERMINATION

The normalized times t_{ONB}^* , t_{CHF}^* , Δt^* , are associated with their uncertainty δt^* defined as

$$\delta t^* = \sqrt{(\delta t_t^*)^2 + \sigma^2} \quad (8)$$

δt_t^* is the uncertainty due to the time resolution of the high-speed IR camera. The frame rate of the camera being 2500, $\delta t_t^* = 0.4ms/\tau$. σ is the standard deviation of the three repetitions of each experiment.